Multi-Objective Mobile Damped Wave Algorithm (MOMDWA): A Novel Approach For Quantum System Control

Juntao Yu [a, +], Jiaquan Yu [a, +], Dedai Wei[b], Xinye Sha[c], Shengwei Fu[d], Minyu Qiu[e], Yurun Jin[f], Kaichen OuYang [a, *]

[a]Department of Mathematics, University of Science and Technology of China, Hefei 230026, China
{tomsnake, xk20031012, oykc}@mail.ustc.edu.cn
[b]College of Economics, Shenyang University, Shenyang 110000, China
wdd31212@163.com
[c]Graduate School of Arts and Sciences, Columbia University, NY 10027, United States of America
xs2399@columbia.edu
[d]Key Laboratory of Advanced Manufacturing Technology, Ministry of Education, Guizhou University, Guiyang 550025, China
shengwei_fu@163.com
[e]China Jiliang University Information Engineering College Hangzhou, Zhejiang, China
vpn2733@autuni.ac.nz
[f]School of Computer Science and Technology, University of Science and Technology of China, Hefei 230026, China
yurunjin@mail.ustc.edu.cn

Abstract. In this paper, we introduce a novel multi-objective optimization algorithm, the Multi-Objective Mobile Damped Wave Algorithm (MOMDWA), specifically designed to address complex quantum control problems. Our approach extends the capabilities of the original Mobile Damped Wave Algorithm (MDWA) by incorporating multiple objectives, enabling a more comprehensive optimization process. We applied MOMDWA to three quantum control scenarios, focusing on optimizing the balance between control fidelity, energy consumption, and control smoothness. The results demonstrate that MOMDWA significantly enhances quantum control efficiency and robustness, achieving high fidelity while minimizing energy use and ensuring smooth control pulses. This advancement offers a valuable tool for quantum computing and other domains requiring precise, multi-objective control.

Keywords: Multi-Objective Optimization, Quantum Control, Multi-Objective Mobile Damped Wave Algorithm.

---

* Corresponding author, + Equal contribution.

1   Introduction

In real-world scenarios, optimization problems are often multifaceted and multidimensional, requiring the simultaneous consideration of conflicting objectives [1]. Focusing on a single objective may overlook other critical factors, limiting the overall solution's effectiveness. While single-objective optimization can yield good results in specific areas, it fails to capture the complexity of the problem as a whole. In contrast, multi-objective optimization offers a more comprehensive approach by balancing and integrating various objectives, leading to more effective problem-solving and improved decision-making.

In multi-objective optimization, conflicting objectives make it challenging to satisfy all goals with a single solution [2]. This requires finding a set of solutions, known as the Pareto optimal set, where no objective can be improved without worsening another. These solutions form the Pareto front, representing the best trade-offs among the objectives. The main advantage of the Pareto optimal set is that it offers a range of optimal solutions, providing decision-makers with flexibility in addressing trade-offs. This approach maximizes the optimization of various goals, enabling a more comprehensive resolution of complex problems.

Multi-objective optimization problems are highly complex, requiring effective solution methods. Metaheuristic approaches, such as multi-objective evolutionary algorithms, swarm intelligence algorithms, and cooperative metaheuristics, have become essential for approximating the Pareto optimal set within a reasonable time [3]. Among these, multi-objective swarm intelligence algorithms stand out for their efficiency and widespread application in solving complex problems. They deliver robust solutions, making them a crucial tool for multi-objective optimization in practical scenarios [4].

Several key swarm intelligence algorithms have proven highly effective in multi-objective optimization. Notably, NSGA-II (Non-dominated Sorting Genetic Algorithm II) uses a Non-dominated Sorting mechanism to maintain diversity and prevent premature convergence, efficiently balancing multiple objectives. Following NSGA-II, MOPSO (Multi-Objective Particle Swarm Optimization) extends Particle Swarm Optimization with Pareto dominance [5]. Other algorithms include MOGWO (Multi-Objective Grey Wolf Optimizer) [6], MOHS (Multi-Objective Harmony Search) [7], MOMVO (Multi-Objective Multi-Verse Optimizer) [8], MOABC (Multi-Objective Artificial Bee Colony) [9], MOGA (Multi-Objective Genetic Algorithm) [10], and MSSA (Multi-Objective Salp Swarm Algorithm) [11]. Each of these algorithms leverages unique strategies to effectively address complex multi-objective problems, showcasing the flexibility and power of swarm intelligence [12].

Quantum information science, a critical frontier in modern technology, combines quantum mechanics with information theory to revolutionize information processing [13, 14]. By leveraging quantum superposition and entanglement, it surpasses classical computing limitations, enabling polynomial-time solutions for complex tasks and marking a paradigm shift in computational complexity. Many challenges in this field are quantum control problems, where precise manipulation of quantum systems is essential for achieving specific states or operations. Effective quantum control enhances the reliability and efficiency of quantum computing, making it a cornerstone of quantum information processing.

In control problems, balancing fidelity, energy [15], and smoothness [16]is crucial. For example, in robotic arm control, high precision and efficiency often require significant energy, while smooth motion is needed to avoid vibrations [16]. Similarly, drone path planning must balance accuracy and energy consumption, optimizing smooth turns and speed for stability and safety.

While not all quantum control problems fit neatly into a multi-objective optimization framework, many do involve trade-offs that can be modeled this way [17]. For instance, in quantum control, the aim is to optimize control fields to transition a quantum system from an initial to a target state, balancing objectives such as maximizing fidelity, minimizing control field intensity, and maintaining smoothness within a limited time. By considering these conflicting objectives together, quantum control problems can be modeled as multi-objective optimization problems [18]. Researchers can use multi-objective optimization methods to find the best balance among these objectives, thereby enhancing the reliability and efficiency of quantum computing. This approach is not only vital in quantum information processing but also widely applicable to other fields that require precise control.

The No Free Lunch theorem asserts that no single algorithm is universally optimal for all problems, which justifies the creation of a multi-objective variant of newer algorithms. This work focuses on an a posteriori algorithm by proposing the multi-objective version of a recently-proposed metaheuristic called the Movable Damped Wave Algorithm (MDWA). The MDWA addresses global optimization problems by mathematically simulating the waveform behavior caused by oscillation phenomena. It begins with multiple initial random solutions and updates them using a mathematical model based on the damped wave function, effectively achieving robust solutions and quickly converging to the global optimum. Although MOMDWA is not a traditional evolutionary algorithm, its optimization process reflects evolutionary principles similar to those found in evolutionary algorithms. MOMDWA iteratively improves solutions, which is akin to the selection, mutation, and recombination processes in evolutionary algorithms. Therefore, the optimization process of MOMDWA exhibits evolutionary characteristics that align with the basic ideas of evolutionary algorithms. Notably, MOMDWA has demonstrated outstanding performance in specific domains such as quantum system control, where traditional evolutionary algorithms may not be as suitable. Thus, the application of MOMDWA in these particular fields highlights its unique value. In conclusion, while MOMDWA is not a traditional evolutionary algorithm, its evolutionary behavior, commonality in multi-objective optimization, effectiveness in specific domains, complementarity with evolutionary algorithms, and promotion of innovation and adaptability all underscore its significance and value in the field of multi-objective optimization.

The rest of the paper is structured as follows: Section 2 introduces the mathematical models of MOMDWA. Sections 3 and 4 detail the quantum control problem we aim to optimize, followed by the experimental results presented in Section 5. Finally, Section 6 concludes the paper.

2   Multi-Objective Mobile Damped Wave Algorithm (MOMDWA)

2.1   Position updating

MOMDWA employs a mutation technique and boundary handling method tailored to different situations. It begins by using a dynamic threshold to influence the mutation and boundary handling methods. Two random numbers, r4 and rand, both between 0 and 1, are used. The choice of mutation method and boundary handling is determined by comparing these random numbers to the dynamic threshold, which is typically set at 0.02.

In the mutation formula, two important parameters are BB and GG. BB is a preset random parameter in [-2, 2], while GG is a random parameter in [0, 1].

The formulas for the two types of mutations are shown in formulas (1) and (2):

$$NEWPOS(i, j) = \left(\frac{a}{BB + POS(i, j)} \times \sin\left(\frac{2\pi}{GG} \times POS(i, j) \right) + rand \times BestX(j) \right) \tag{1}$$

$$POS(i, j) = BestX(j) + rand \times 0.95^{gen} \tag{2}$$

2.2   boundary checking and handling

As for boundary process, we use a dynamic threshold to handle this problem. Normally, the threshold is set to 0.02. Then we compare a random number to the threshold. If this random number is larger than the threshold. The formulas are shown in (3).

$$\begin{cases} POS_i(j) = VAR_1(j) & POS_i(j) > VAR_1(j) \text{ and } POS_i(j) > VAR_2(j), \\ POS_i(j) = VAR_1(j) + VAR_2(j) & POS_i(j) > VAR_1(j) \text{ and } POS_i(j) < VAR_2(j), \\ POS_i(j) = POS_i(j) & POS_i(j) < VAR_1(j) \text{ and } POS_i(j) > VAR_2(j), \\ POS_i(j) = VAR_2(j) & POS_i(j) < VAR_1(j) \text{ and } POS_i(j) < VAR_2(j) \end{cases} \tag{3}$$

If not, then the formulas are like (4).

$$\begin{cases} POS_i(j) = POS_i(j) & POS_i(j) < VAR_1(j) \text{ and } POS_i(j) > VAR_2(j), \\ POS_i(j) = random(VAR_1(j), VAR_2(j)) & \text{Otherwise.} \end{cases} \tag{4}$$

2.3   non-dominated sorting and crowding distance mechanism

MOMDWA uses non-dominated sorting and a diversity-preserving crowding distance mechanism to achieve better results. Non-dominated sorting involves three steps:

- First, calculating the non-dominated solution with objective values.
- Second, applying non-dominated sorting (NDS) and dividing solutions into levels based on dominance. The first level includes all non-dominated solutions, which are removed, and the process is repeated for the remaining solutions.

- Calculating non-dominated ranking (NDR) of all non-dominated solutions.

Crowding Distance measures how "crowded" a solution is in a multi-objective space, aiming to maintain diversity and avoid premature convergence. It is calculated by first sorting the objective function values. The crowding distance for boundary solutions is set to infinity, prioritizing them, while for non-boundary solutions, it is calculated using the following formula:

$$CD_i^j = \frac{f_{i+1}^j - f_{i-1}^j}{f_{max}^j - f_{min}^j} \tag{5}$$

where CD_i^j represents the crowding distance of solution i for objective j. This metric identifies solutions in different regions of the objective space, preserving diversity.

2.4   Multi-Objective Mobile Damped Wave Algorithm (MOMDWA)

The MOMDWA algorithm starts by initializing the population, checking for dominated particles, and calculating the non-dominated rank (NDR) to identify non-dominated fronts. A grid is then generated for the solution space. The algorithm updates particle positions, checks and handles boundaries, and updates the objective space. After updating the repository and deleting excess particles, the algorithm checks whether to repeat the position update step. If necessary, the loop continues; otherwise, the algorithm ends.
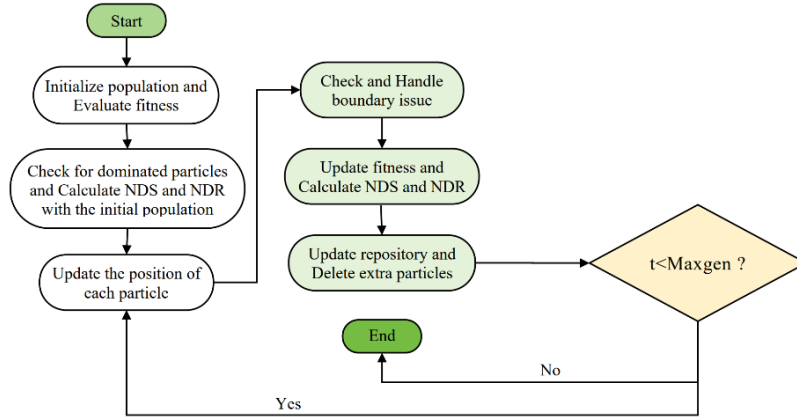
The whole process of the algorithm is demonstrated in the following pseudocode and flow charts in Fig. 1.

Algorithm 1 Pseudocode for the Algorithm

1: **STEP 1: Population Initialization, Fitness Evaluation and Check Domination Relationship**
2: POS = repmat((var_max - var_min)', Np, 1) .* rand(Np, dim) + repmat(var_min', Np, 1);
3: Fitness = fobj(POS);
4: Check domination relationship of each particle, perform Non-dominated sort, and calculate Non-dominated rank.
5: **STEP 2: Updating the Position of Each Particle**
6: BestX = select a random particle from the REP;
7: **if** rand < threshold **then**
8:    $NEWPOS(i,j) = \frac{a}{BB+POS(i,j)} \times \sin\left(\frac{2\pi}{GG} \times POS(i,j)\right) + rand \times BestX(j)$
9: **else**
10:    $NEWPOS(i,j) = BestX(j) + rand \times 0.95^{gen}$
11: **end if**
12: **STEP 3: Boundary Checking and Handling**
13: **if** rand > threshold **then**
14:

   case 1: $POS_i(j) = VAR_1(j)$ $POS_i(j) > VAR_1(j)$ $POS_i(j) > VAR_2(j)$;
   case 2: $POS_i(j) = VAR_1(j) + VAR_2(j)$ $POS_i(j) > VAR_1(j)$ $POS_i(j) < VAR_2(j)$;
   case 3: $POS_i(j) = POS_i(j)$ $POS_i(j) < VAR_1(j)$ $POS_i(j) > VAR_2(j)$;
   case 4: $POS_i(j) = VAR_2(j)$ $POS_i(j) < VAR_1(j)$ $POS_i(j) < VAR_2(j)$.
15: **else**
16:

   case 1: $POS_i(j) = POS_i(j)$ $POS_i(j) < VAR_1(j)$ $POS_i(j) > VAR_2(j)$;
   case 2: $POS_i(j) = random(VAR_1(j), VAR_2(j))$ $Otherwise$.
17: **end if**
18: **STEP 4: Updating Fitness and Upgrade REP**
19: Evaluate the fitness of each particle;
20: Check domination relationship and calculate NDS and NDR;
21: Update the REP.
22: **STEP 5: Deleting Excessive Particles**
23: Calculate crowding distance of each particle;
24: Delete the particles with the smallest crowding distance;
25: Move back to STEP 2 until iteration reaches the maximum.

Fig. 1. Flow Charts of MOMDWA

2.5 The relationship between MOMDWA and Evolutionary Algorithms

Although the core mechanism of MOMDWA is derived from the propagation and attenuation process of physical waves, it shares many commonalities with evolutionary algorithms in terms of behavior and functionality. Evolutionary algorithms simulate the natural evolution process, gradually approaching the optimal solution through the

evolution, selection, mutation, and crossover of a population. Similarly, MOMDWA simulates the evolution and optimization of a solution set by propagating and adjusting waves in the solution space. The following Table 1 demonstrates the relationship between MOMDWA and Evolutionary Algorithms.

Table 1. the relationship between MOMDWA and Evolutionary Algorithms.

Commonality	MOMDWA Mechanism	Evolutionary Algorithm Mechanism
Population Evolution	Simulates the diffusion and evolution of solutions in the solution space through damped wave propagation.	Achieves individual evolution and adaptation through selection, crossover, and mutation of the population.
Fitness Evaluation and Environmental Feedback	Uses multi-objective optimization criteria (such as fidelity, energy consumption, smoothness) to assess solution fitness, similar to the fitness function in evolutionary algorithms.	Uses a fitness function to evaluate individual fitness, determining their survival in the population.
Selection and Elimination	Selects well-performing solutions through non-dominated sorting and crowding distance mechanisms, eliminating poorer solutions.	Selects superior individuals based on fitness, and eliminates less fit individuals through selection, crossover, and mutation.
Mutation and Diversity Maintenance	Introduces random mutation and dynamic parameter control to maintain diversity of solutions, preventing local optima.	Introduces individual diversity through crossover and mutation mechanisms, avoiding premature convergence.
Global Exploration and Local Exploitation	Balances global exploration and local exploitation through wave propagation and reflection.	Combines global search (via crossover) and local search (via mutation) to thoroughly explore the solution space.
Multi-objective Optimization and Pareto Front	Constructs the Pareto front through non-dominated sorting and wave superposition mechanisms, finding the optimal balance of multiple objectives.	Identifies solutions on the Pareto front through non-dominated sorting in multi-objective optimization.
Gradual Convergence and Optimization	Solutions gradually converge to the optimal region as wave amplitude decreases.	Individuals gradually converge to the optimal solution over generations.
Simulation of Natural Phenomena	Simulates the phenomenon of damped wave propagation for solution updating and optimization, akin to the natural selection process in evolutionary algorithms.	Simulates natural evolutionary processes such as selection, crossover, and mutation.

This comparison table highlights the deep-seated commonalities between MOMDWA and evolutionary algorithms. Although MOMDWA is inspired by the physical phenomenon of damped wave propagation, it exhibits evolutionary behavior similar to that of evolutionary algorithms when addressing multi-objective optimization problems. By simulating natural wave propagation and attenuation processes, MOMDWA effectively explores, selects, and optimizes in the solution space, ultimately finding the optimal solution that balances multiple conflicting objectives. Both algorithms demonstrate common strategies in handling solution diversity, balancing global search and local optimization, and making trade-offs in multi-objective optimization. This makes MOMDWA not only capable of inheriting the strengths of evolutionary algorithms but also of offering new optimization pathways through its unique wave mechanism, providing a powerful solution for multi-objective optimization problems.

3   Problems of Quantum Control

Quantum system control involves precisely manipulating the dynamics of a quantum system by adjusting external control fields to achieve desired quantum states or operations. Effective quantum control enhances the reliability and efficiency of quantum computation, making it crucial for quantum information processing. Multi-objective optimization algorithms can solve quantum control problems by adjusting control fields to transition a quantum system from an initial state to a target state, optimizing control functions related to field strength and timing to reach the best possible state within a given timeframe.

Key optimization objectives include fidelity, control field strength (energy consumption), and control field smoothness. In scientific research and engineering, various quantum control models target systems like atoms in multi-level structures or qubits in superconducting circuits [17]. Despite differing physical characteristics, a quantum system's state is generally described by a quantum state $|\psi(t)\rangle$, a complex vector defined by the system's specific physical properties. The quantum state evolution follows the Schrödinger equation (6).

$$i\hbar \frac{d}{dt}|\psi(t)\rangle = H(t)|\psi(t)\rangle \tag{6}$$

The Hamiltonian $H(t)$ is derived from the system's energy level structure and external control fields, comprising the Hamiltonians of free, coupling, and external control fields. For a quantum system with M external control fields and F free and coupling fields as is shown in equation (7).

$$H(t) = \sum_{m=1}^{M} u_m(t)H_m + \sum_{f=1}^{F} H_f \tag{7}$$

Here, $u_m(t)$ represents the control functions, H_m is the Hamiltonian of the control field, and H_f is the Hamiltonian of the free and coupling fields. Many quantum systems

are uncertain, carrying random parameters $\{\theta_i\}_{i=1}^{M+F}$ (fixed during control but random during each control). These parameters affect the Hamiltonian via influence functions $\{f_i(t;\theta_i)\}_{i=1}^{M+F}$, thereby influencing the evolution of the quantum state as in shown equation (8).

$$H(t) = \sum_{m=1}^{M} u_m(t) f_m(t;\theta_m) H_m + \sum_{f=1}^{F} f_{M+f}(t;\theta_{M+f}) H_f \tag{8}$$

The quantum system's control objective is to adjust control functions $u_m(t)_{(m=1)}^{M}$ so that the final quantum state $|\psi(T)\rangle$ closely matches the target state $|\psi_{\text{target}}\rangle$ within the time T. A performance function $J(u)$ is defined to evaluate the control strategy's quality, usually in terms of fidelity or the distance in complex space between the final and target states. The goal is to find the optimal the value of control functions that minimizes or maximizes $|\psi(T)\rangle$.

3.1   State Preparation in V-Type Three-Level Quantum Systems

A V-type three-level quantum system is a key model in quantum mechanics, consisting of three energy levels with two higher levels coupled to a common lower level. This system is crucial for understanding light-matter interactions, quantum interference, and coherence, which are essential for quantum information processing and computing. It finds applications in qubit operations, quantum gates, entangled state generation, single-photon sources, high-precision spectroscopy, and laser design, especially for multi-frequency lasers.

In quantum system with uncertainties, initialization, state evolution and target state of control are key steps for achieving quantum state control. As for initial state, it is usually the ground state in equation (9):

$$|\psi(0)\rangle = | g\rangle, \ \Psi(0) = (1, 0, 0) \tag{9}$$

and the target state is typically a superposition state shown in equation (10):

$$|\psi_{\text{target}}\rangle = \frac{1}{\sqrt{2}} | e_1\rangle + \frac{1}{\sqrt{2}} | e_2\rangle, \ \Psi_{\text{target}} = \left(0, \frac{1}{\sqrt{2}}, \frac{1}{\sqrt{2}} \right) \tag{10}$$

The evolution of the state of a quantum system is determined by the Schrödinger equation, and the key elements in Schrödinger equation is the Hamiltonian. The Hamiltonian in this problem is derived from the contribution of one free field and four external control fields as is shown in equation (11):

$$H(t) = f_0(t;\theta_0) H_0 + \sum_{m=1}^{4} u_m(t) f_m(t;\theta_m) H_m \tag{11}$$

Where H_0 is the free Hamiltonian, and the control Hamiltonians are $H_i, i = 1,2,3,4$. The formula of them are shown in shown in equation (12).

$$H_0 = \begin{pmatrix} 1.5 & 0 & 0 \\ 0 & 1 & 0 \\ 0 & 0 & 1 \end{pmatrix}, H_1 = \begin{pmatrix} 0 & 1 & 0 \\ 1 & 0 & 0 \\ 0 & 0 & 0 \end{pmatrix}, H_2 = \begin{pmatrix} 0 & -i & 0 \\ i & 0 & 0 \\ 0 & 0 & 0 \end{pmatrix}, H_3 = \begin{pmatrix} 0 & 0 & 1 \\ 0 & 0 & 0 \\ 1 & 0 & 0 \end{pmatrix}, H_4 = \begin{pmatrix} 0 & 0 & -i \\ 0 & 0 & 0 \\ i & 0 & 0 \end{pmatrix} \quad (12)$$

These are designed based on quantum control theory, Lie algebras, and the Lyapunov control method, starting from the generators of the $SU(3)$ group. The influence function for the uncertainty parameters is given by $f_0(t; \theta_0) = 1 - \epsilon \theta \cos t$, $f_i(t; \theta_i) = 1$, $i = 1,2,3,4$, where ϵ is an inherent parameter of the quantum system.

3.2   Superconducting Quantum Circuits

Superconducting quantum circuits, based on Josephson junctions, demonstrate quantum behavior similar to artificial atoms, making them vital for quantum computing and quantum information processing [21]. Their flexibility and scalability enable the construction of qubits, the fundamental units of quantum computing, with the potential for large-scale integration due to long coherence times and high operational precision. These circuits are key in validating fundamental principles of quantum mechanics, crucial for both applied and fundamental research [22].

In superconducting quantum circuits, two primary types of qubits—flux qubits and charge qubits—are controlled by adjusting external parameters like magnetic flux Φ and gate voltage V_g [23]. The basic Hamiltonian for charge qubits is given by equation (13).

$$H = F_z(V_g)\sigma_z - F_x(\Phi)\sigma_x \quad (13)$$

Here $F_z(V_g)\sigma_z$ and $F_x(\Phi)\sigma_x$ are respectively related to the charging energy E_C and E_J, which can be adjusted by external parameters such as the voltage V_g and the magnetic flux Φ. Meanwhile σ_z and σ_x are Pauli matrices.

In more complex operations, coupled two-qubit systems use an LC oscillator, leading to a Hamiltonian of the form in equation (14):

$$H = \sum_{i=1}^{2} \left[F_z(V_i)\sigma_z(i) + F_x(\Phi_i)\sigma_x(i) \right] + \chi(\gamma)\sigma_z(1) \otimes I(2). \quad (14)$$

After normalization and simplification, the expression of Hamiltonian is shown in equation (15):

$$\frac{H}{\hbar} = \theta_1 u_1(t)\sigma_\zeta(1) \otimes I(2) + \theta_2 u_2(t)\sigma_\zeta(1) \otimes \sigma_\zeta(2) - \theta_3 u_3(t)\sigma_x(1) \otimes I(2)$$
$$- \theta_4 u_4(t)\sigma_x(1) \otimes \sigma_\zeta(2) - \theta_5 u_5(t)\sigma_y(1) \otimes \sigma_y(2) \quad (15)$$

In the normalized Hamiltonian formula, θ_m represents coefficients of uncertainty

parameters with specific values varying within a given range, while $u_i(t)$ are control functions used to manipulate the state of the qubits. This formulation expresses the system's Hamiltonian in a simplified form that includes uncertainty and control parameters, facilitating more convenient control and optimization in practical operations. Where θ_m represents uncertainty coefficients, and $u_i(t)$ are control functions that manipulate the qubits' states.

The initial state of control is the ground state as is shown in equation (16).

$$|\psi(0)\rangle = |g_1 g_2\rangle, \quad \Psi(0) = (1,0,0,0) \tag{16}$$

and the target state of control is the maximally entangled state as is shown in equation (17).

$$|\psi_{\text{target}}\rangle = \frac{1}{\sqrt{2}}(|g_1 e_2\rangle + |e_1 g_2\rangle), \Psi_{\text{target}} = \left(0, \frac{1}{\sqrt{2}}, \frac{1}{\sqrt{2}}, 0\right) \tag{17}$$

3.3 A quantum system consisting of two two-level atoms

The quantum system of two two-level atoms interacting with a quantized field in a cavity is widely used in experimental quantum optics and information processing, offering key insights into entangled state dynamics. Controlling entanglement between atoms is vital for quantum communication and computation, enabling tasks like teleportation, key distribution, and gate operations. Effective control ensures high-fidelity generation and manipulation of entangled states, essential for robust quantum computing and secure communication [24].

The Hamiltonian governing the dynamics of this system comprises contributions from the free evolution of the atoms and the field, the interaction between the atoms, and the interaction between the atoms and the field [25]. It is expressed as equation (18).

$$H(t) = H_0 + H_I + H_u \tag{18}$$

where:

H_0 represents the energy of the atoms and the field,

H_I denotes the interaction between the atoms and the interaction between the atoms and the field,

H_u is the control Hamiltonian, which allows for the manipulation of the system's state through external controls.

The specific forms of these Hamiltonians are in equation (19), (20) and (21).

$$H_0 = \frac{1}{2}\sum_{i=1}^{2}\omega_{A_i}\sigma_z^{(i)} + \omega_r a^? a, \tag{19}$$

$$H_I = \sum_{i \neq j}\Omega_{ij}\sigma_+^{(i)} \otimes \sigma_-^{(j)} + \sum_j \nu_j\left(a^?\sigma_-^{(j)} + a\sigma_+^{(j)}\right), \tag{20}$$

$$H_u = \sum_{i=1}^{2} u_{\omega_{A_i}}(t)\sigma_z^{(i)} + u_{\omega_r}(t)a^?a + \sum_{i \neq j} u_{\Omega_{ij}}(t)\sigma_+^{(i)} \otimes \sigma_-^{(j)} + \sum_{j} u_{\nu_j}(t)\left(a^?\sigma_-^{(j)} + a\sigma_+^{(j)}\right). \qquad (21)$$

Here, ω_{A_i} and ω_r are the atomic transition frequencies and the field frequency, respectively; Ω_{ij} is the dipole-dipole interaction parameter; and ν_j is the coupling constant between the atoms and the quantized field. The control problem involves driving the system from an initial ground state as is shown in equation (22).

$$|\psi(0)\rangle = |g_1g_2\rangle, \ \Psi(0) = (1,0,0,0) \qquad (22)$$

where both atoms are in their ground states, to a target maximally entangled state as is shown in equation (23).

$$|\psi_{\text{target}}\rangle = \frac{1}{\sqrt{2}}(|g_1e_2\rangle + |e_1g_2\rangle), \Psi_{\text{target}} = \left(0, \frac{1}{\sqrt{2}}, \frac{1}{\sqrt{2}}, 0\right) \qquad (23)$$

4   Quantum Control Using Optimization Algorithms

4.1   Search Space of Optimization Algorithm and Numerical Solution of Quantum System

The control functions u of the quantum system are the variables solved by the optimization algorithm, mapped to the algorithm's search space through grid sampling. We uniformly take N sample points, corresponding to times $\{t_0, t_1, \cdots, t_N\} = \{0, \frac{T}{N}, \frac{2T}{N}, \cdots, \frac{(N-1)T}{N}, T\}$, where T is the total control time. The values of each control function at the first N points form the search space of the optimization algorithm. If there are M control functions, the search space has $M \times N$ dimensions, meaning a particle in the optimization algorithm is in equation (24).

$$Pos(i) = \{u_1(t_0), u_1(t_1), \cdots, u_1(t_{N-1}), u_2(t_0), u_2(t_1), \cdots, u_2(t_{N-1}), \cdots, u_M(t_0), u_M(t_1), \cdots, u_M(t_{N-1})\} \quad (24)$$

Given the value of control functions and uncertain parameters, we can use the finite difference method to solve the Schrödinger equation and calculate the system's state Ψ of the system at these sample points; that is, for the Schrödinger equation like (25).

$$i\hbar \frac{d}{dt}|\psi(t)\rangle = H(t)|\psi(t)\rangle = \left(\sum_{i=1}^{M} u_i(t)f_i(t;\theta_i)H_i(t) + \sum_{j=M+1}^{M+F} f_j(t;\theta_j)H_j(t)\right)|\psi(t)\rangle \qquad (25)$$

Here, in equation (25), $\{u_i(t)\}_{i=1}^{M}$ are the control functions, $\{f_i(t;\theta_i)\}_{i=1}^{M+F}$ are the influence functions of the uncertain parameters, and $\{H_i(t)\}_{i=1}^{M+F}$ are the Hamiltonians. Using the finite difference method for numerical calculations, the states $\{\Psi(t_i)\}_{i=0}^{N}$ at

the sample points follow the recursion formula (26).

$$\Psi(t_{i+1}) = \Psi(t_i) + \frac{d}{dt}\Psi(t_i)\Delta t = \Psi(t_i) - \frac{i}{\hbar}H(t_i)\Psi(t_i)\Delta t \tag{26}$$

This allows us to calculate the state $\{\Psi(t_i)\}_{i=0}^N$ of the system over the entire control time T.

If the sample points are too few, the finite difference method's numerical error increases; too many points, and the optimization algorithm's search space becomes too large. To address this, we use spline interpolation. Assuming the number of sample points in the search space is N, we interpolate the value of control functions $\{u_i(t_j)\}_{j=0}^{N-1}$ to $\{u_i(t_j,)\}_{j=0}^{\alpha(N-1)}$, where α is our interpolation factor, and $\{t_j,\}_{j=0}^{\alpha(N-1)}$ are the uniformly sampled points by taking αN as the sampling number. This ensures numerical accuracy while keeping the search space manageable.

4.2   Optimization Objectives of Multi-objective Optimization Algorithm

Performance Function. The primary optimization objective is the performance function $J(u)$, usually defined as fidelity, which is based on the final state $\Psi(T)$ of the quantum system and the target state Ψ_{target}. We aim to maximize this fidelity, typically calculated as the square of the modulus of the inner product of these two states for pure quantum states as is shown in equation (27).

$$J(u) = Fidelity = |\langle \Psi(T) | \Psi_{\text{target}} \rangle|^2 \tag{27}$$

For mixed quantum states, it is the trace distance between the two states. First, we calculate the density matrices $\rho(T)$ and ρ_{target} of the two states as is shown in equation (28).

$$\rho(T) = |\Psi(T)\rangle\langle\Psi(T)|, \quad \rho_{\text{target}} = |\Psi_{\text{target}}\rangle\langle\Psi_{\text{target}}| \tag{28}$$

then calculate the trace distance between the two density matrices as is shown in equation (29).

$$J(u) = Fidelity = Tr\left(\sqrt{\sqrt{\rho(T)}\,\rho_{\text{target}}\sqrt{\rho(T)}}\right). \tag{29}$$

In the three quantum control problems mentioned, the first two involve pure states, while the third involves a mixed state. Fidelity, defined by the alignment of vectors in complex space, is maximized when the final state and target state are aligned or opposite. However, this can lead to optimization challenges, as optimal solutions may cluster in two distant areas of the search space, complicating convergence. To address this, we use the distance deviation between quantum states as the optimization objective instead of fidelity, measuring performance by the distance in complex space, as is shown in equation (30).

$$J(u) = Deviation = \| \Psi(T) - \Psi_{\text{target}} \| \tag{30}$$

For mixed quantum states, as is shown in equation (31).

$$J(u) = Deviation = \| \rho(T) - \rho_{\text{target}} \| \tag{31}$$

Our optimization goal is to minimize or maximize Deviation, which we refer to as positive fidelity optimization and negative fidelity optimization, respectively.

Energy Consumption. In quantum control optimization, besides maximizing fidelity, energy consumption, which reflects the cost of control, must also be considered [15]. We define the energy consumption objective function as the equation (32).

$$Energy = \sum_{i=1}^{M} \int_{0}^{T} |u_i(t)| \cdot \| H_i(t) \| \, dt = \sum_{i=1}^{M} \sum_{j=1}^{N} |u_i(t_j)| \cdot \| H_i(t_j) \| \cdot \Delta t, \tag{32}$$

Where M is the number of control fields, N is the number of sample points in the numerical calculation, and $\Delta t = \dfrac{T}{N}$ is the time interval between sample points.

Smoothness of Control Pulses. In quantum control, pulse smoothness is crucial to reduce high-frequency noise and non-ideal effects. We introduce an objective function to measure this smoothness, in other word, the sharp changes in control pulses over time [26]. It is calculated by the integral of the square of their first derivative [16]. Specifically, let $U_i(t) = |u_i(t)| \cdot \| H_i(t) \| \, (i=1,2,\cdots,m)$, then the smoothness objective function of control pulses is defined as equation (33).

$$Smoothness = \sum_{i=1}^{M} \int_{0}^{T} \left(\frac{dU_i(t)}{dt} \right)^2 dt = \sum_{i=1}^{M} \sum_{j=1}^{N-1} \left(\frac{U_i(t_{j+1}) - U_i(t_j)}{\Delta t} \right)^2 \Delta t. \tag{33}$$

The quantity we define is negatively correlated with control smoothness.

We use a multi-objective optimization algorithm to simultaneously optimize three objectives: achieving high fidelity in quantum control, minimizing energy consumption, and improving control system efficiency and sustainability. This also ensures smoother control pulses, reduces high-frequency noise and non-ideal effects, stabilizes the system, and makes control easier to implement.

4.3   TOPSIS Evaluation

Using the multi-objective optimization algorithm MOWDOA, we obtain a repository representing viable control function values with no dominance relationships. To select the 'optimal solution,' we apply the TOPSIS algorithm to evaluate the solutions on the Pareto front.

We start by screening the solutions based on fidelity, as other metrics like energy

consumption and control smoothness are irrelevant if fidelity is too low. Solutions above the fidelity threshold proceed to TOPSIS. We construct a matrix including values for each objective function (Size × MultiNum dimensions) and normalize the data positively, where for each objective function value $fobj_{ij}$, let $fobj_{ij} \leftarrow max(fobj_{ij}) - fobj_{ij}$, since larger values receive higher scores in the TOPSIS algorithm. We then calculate the distance between each solution's objective function vector and the vectors formed by the maximum and minimum values of each objective function as is shown in equation (34).

$$D_i^+ = \sqrt{\sum_{j=1}^{MultiNum} W_j(fobj_{ij} - fobj_j^+)^2}, \quad D_i^- = \sqrt{\sum_{j=1}^{MultiNum} W_j(fobj_{ij} - fobj_j^-)^2}, \tag{34}$$

We set weight coefficients $\{W_j\}_{j=1}^{MultiNum}$ to adjust the importance of each objective function. We then calculate the comprehensive score for each solution to obtain the score array $\{S_i\}_{i=1}^{Size}$ as is shown in equation (35).

$$S_i = \frac{D_i^-}{D_i^+ + D_i^-}. \tag{35}$$

Finally, we normalize the score array $\{S_i\}_{i=1}^{Size}$ to obtain the final score results. After sorting, we can select the optimal solution.

5   Numerical Experiment

We used the MOMDOA algorithm for both bi-objective and tri-objective optimizations in three quantum control problems. The bi-objective targets were performance function and energy dissipation, while the tri-objective added control smoothness. Auxiliary parameters included interpolation factor $\alpha = 30$, fidelity truncation threshold $\varepsilon = 0.995$, and the TOPSIS evaluation weights $(W_{Fidelity}, W_{Energy}) = (0.7, 0.3)$ for two objectives, and $(W_{Fidelity}, W_{Energy}, W_{Smoothness}) = (0.6, 0.2, 0.2)$ for three objectives.

Table 2 and Table 3 show the results: curvature and Pareto front, optimal control function u, its distribution, and the evolution of the quantum state Ψ. Table 4 shows the parameters of the MOMDWA used in each problem.

Table 2. double objectives optimization of the quantum control.

	Q1	Q2	Q3
Fidelity	9.99977E-01	9.99902E-01	9.99241E-01
Energy	2.98414E+00	5.44407E+00	8.51772E+01

Table 3. triple objectives optimization of the quantum control.

	Q1	Q2	Q3
elity	9.99690E-01	9.99573E-01	9.98809E-01
Energy	4.14350E+00	5.58225E+00	5.05166E+01
Smoothness	7.56408E+00	1.94418E+01	8.87840E+01

Table 4. parameters in algorithms.

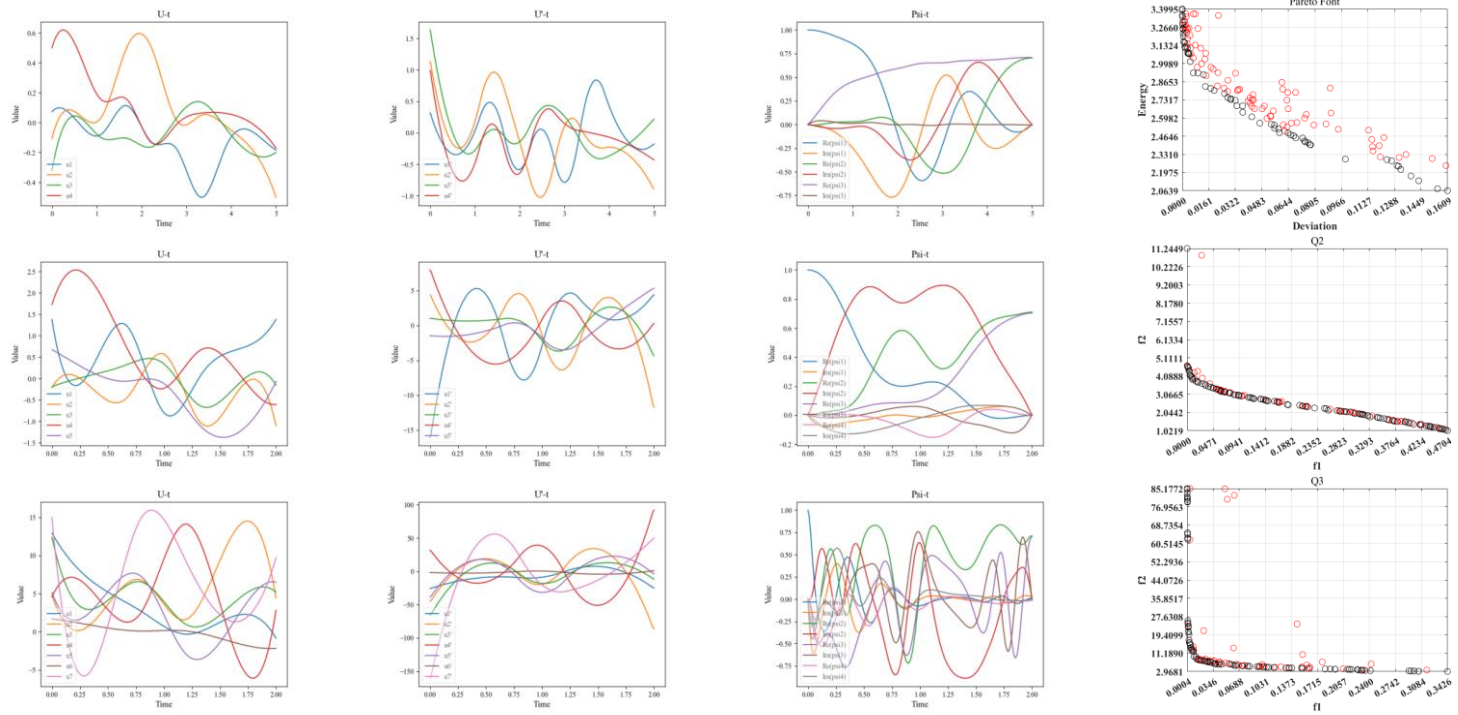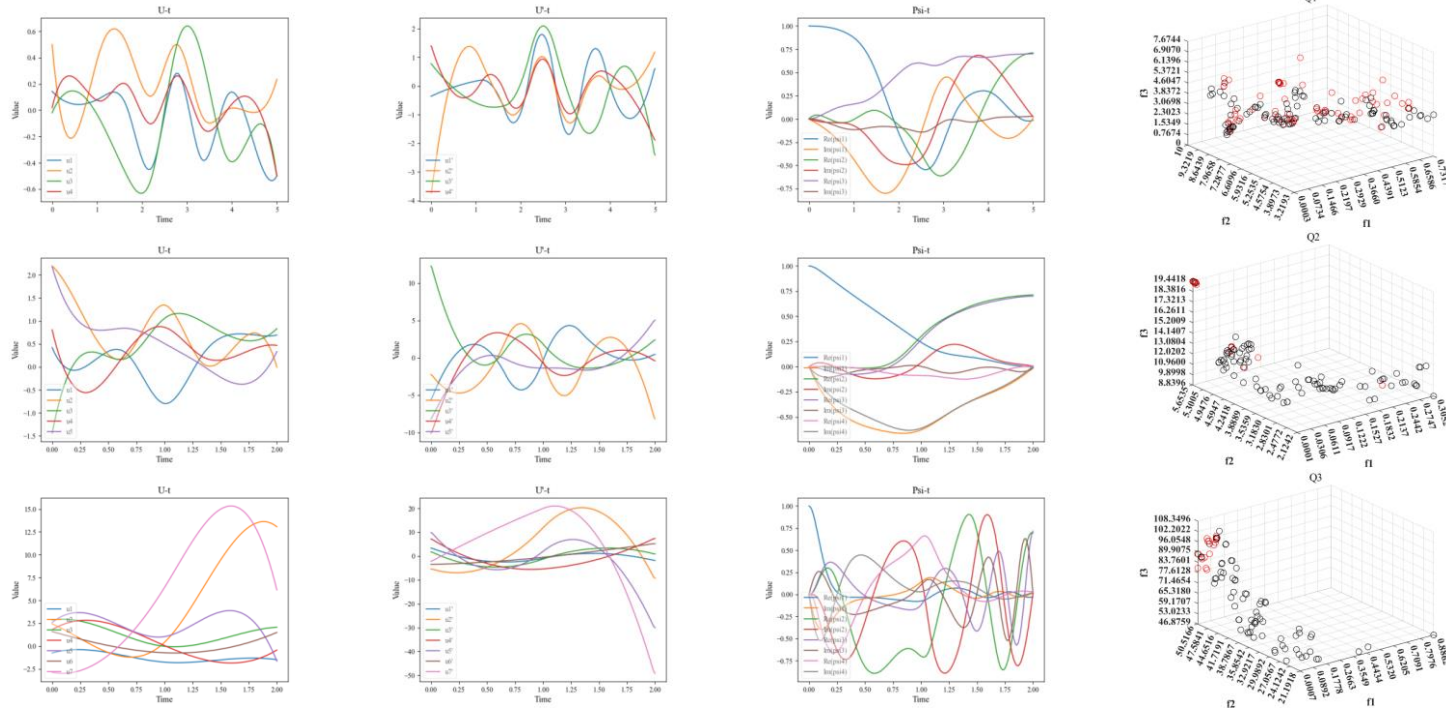|	Population Size	Repository Size	Search Space Demension	Maximum Number of Generations
Q1	100	100	40	500
Q2	100	100	35	500
Q3	100	100	42	500

Fig. 2. the curves in double-objective cases

Fig 3 the curves in triple-objective cases

The Pareto front graph in Fig 2 and Fig 3 shows a well-distributed and smooth curve, highlighting the effectiveness of our algorithm in balancing competing objectives like fidelity, energy consumption, and control smoothness. The desirable shape of the Pareto front indicates that our algorithm successfully finds optimal trade-offs, ensuring high-quality quantum control solutions. This confirms that our method provides a robust set of efficient and reliable strategies tailored for various quantum control needs.

Annotations Q1, Q2, and Q3 represent the state preparation problem in a V-type three-level quantum system, the coupling problem of two qubits in a superconducting quantum circuit, and the coupling problem of two two-level atoms, respectively. Our optimization algorithm achieved quantum control fidelities of 0.9999, 0.9999, and 0.9992 for Q1, Q2, and Q3, respectively—significantly improving fidelity compared to traditional sampling-based learning control algorithms, which achieved fidelities of 0.9961, 0.9992, and 0.9966 [17]. These exciting results are evident in the Psi-t images, where the overlap between the final quantum state obtained by our algorithm and the target state is very high.

Additionally, since we considered a multi-objective optimization algorithm, our algorithm also take account of energy consumption and the smoothness of the control pulses, providing a significant advantage in practical quantum control. In the U-t graph, the small amplitude of the control function indicates low energy consumption, reducing power requirements and minimizing the risk of decoherence in quantum systems. The smoothness of the U-t graph, without sharp fluctuations, highlights high control smoothness—crucial for minimizing noise and errors, ensuring stable and reliable quantum operations.

Similarly, the small amplitude in the U'-t graph further suggests high control smoothness. Smooth control signals enhance the system's robustness against perturbations, helping maintain high fidelity and ensuring the system closely follows the desired trajectory. Overall, the excellent performance of our optimization algorithm on quantum control problems greatly improves efficiency, sustainability, ease of implementation, and robustness of quantum control.

6   Conclusion

This article introduces the single-objective optimization algorithm MDVA and then proposes the multi-objective optimization algorithm MOMDVA based on it. We retained the core characteristics of MDVA and extended it to a multi-objective version, providing a detailed explanation of its mathematical model and corresponding pseudocode. This extension aims to better address multi-objective optimization problems in practical engineering.

Based on theoretical analysis, this paper applies the proposed MOMDVA algorithm to solve three quantum control problems. Techniques were adopted to make our algorithm applicable to quantum control problems, and the results demonstrate that the algorithm performs exceptionally well, verifying its effectiveness and applicability in multi-objective optimization. It significantly improves efficiency, sustainability, ease of implementation, and robustness of quantum control. These findings indicate that the MOMDVA algorithm not only inherits the advantages of MDVA but also offers unique

performance benefits in handling multi-objective problems, particularly in quantum control.

Despite the positive outcomes, this study has limitations. Firstly, the current test set is relatively limited, making it insufficient to fully evaluate the algorithm's universality and stability. Secondly, further exploration of the MOMDVA algorithm's performance in more quantum control and practical engineering problems is needed to verify its adaptability, effectiveness, and feasibility in various domains and real-world environments. Thirdly, the robustness of the algorithm in quantum control problems needs to be thoroughly tested and discussed. Fourthly, there is a need to extend MOMDVA to a dynamic multi-objective version to tackle more complex real-world problems.

Based on these findings, this paper suggests the following directions for future research:

1. Expanding the test set to verify the algorithm's performance on a broader dataset, thereby further assessing its universality and stability.
2. Applying the MOMDVA algorithm to more quantum control and practical engineering problems to explore its adaptability, effectiveness, and feasibility in different domains and real-world environments.
3. Testing and discussing the robustness of the MOMDVA algorithm in quantum control problems.
4. Extending MOMDVA to a dynamic multi-objective version to address and solve more complex real-world challenges.

Through these expansions and improvements, we aim to enhance the practicality and broad application prospects of the MOMDVA algorithm, thereby providing stronger support for the development of multi-objective optimization. We believe that with continued research and optimization, the MOMDVA algorithm will play an increasingly important role in future engineering and scientific applications.

Reference

1. Cruz, C., J.R. González, and D.A. Pelta, *Optimization in dynamic environments: a survey on problems, methods and measures.* Soft Computing, 2011. **15**: p. 1427-1448.
2. Yuan, Y., et al., *Objective reduction in many-objective optimization: evolutionary multiobjective approaches and comprehensive analysis.* IEEE Transactions on Evolutionary Computation, 2017. **22**(2): p. 189-210.
3. Maltese, J., B.M. Ombuki-Berman, and A.P. Engelbrecht, *A scalability study of many-objective optimization algorithms.* IEEE Transactions on Evolutionary Computation, 2016. **22**(1): p. 79-96.
4. Tanabe, R. and H. Ishibuchi, *An easy-to-use real-world multi-objective optimization problem suite.* Applied Soft Computing, 2020. **89**: p. 106078.
5. Coello, C.C. and M.S. Lechuga. *MOPSO: A proposal for multiple objective particle swarm optimization.* in *Proceedings of the 2002 Congress on Evolutionary Computation. CEC'02 (Cat. No. 02TH8600).* 2002. IEEE.
6. Mirjalili, S., et al., *Multi-objective grey wolf optimizer: a novel algorithm for multi-criterion optimization.* Expert systems with applications, 2016. **47**: p. 106-119.

7. Ghanbari, K., A. Maleki, and D.R. Ochbelagh, *Optimal design of solar/wind/energy storage system-powered RO desalination unit: Single and multi-objective optimization.* Energy Conversion and Management, 2024. **315**: p. 118768.

8. Mirjalili, S., et al., *Optimization of problems with multiple objectives using the multi-verse optimization algorithm.* Knowledge-Based Systems, 2017. **134**: p. 50-71.

9. Nasiraghdam, H. and S. Jadid, *Optimal hybrid PV/WT/FC sizing and distribution system reconfiguration using multi-objective artificial bee colony (MOABC) algorithm.* Solar Energy, 2012. **86**(10): p. 3057-3071.

10. Rehman, A., et al., *Multi-objective approach of energy efficient workflow scheduling in cloud environments.* Concurrency and Computation: Practice and Experience, 2019. **31**(8): p. e4949.

11. Mirjalili, S., et al., *Salp Swarm Algorithm: A bio-inspired optimizer for engineering design problems.* Advances in engineering software, 2017. **114**: p. 163-191.

12. Mavrovouniotis, M., C. Li, and S. Yang, *A survey of swarm intelligence for dynamic optimization: Algorithms and applications.* Swarm and Evolutionary Computation, 2017. **33**: p. 1-17.

13. Gebhart, V., et al., *Learning quantum systems.* Nature Reviews Physics, 2023. **5**(3): p. 141-156.

14. Sigov, A., L. Ratkin, and L.A. Ivanov, *Quantum information technology.* Journal of Industrial Information Integration, 2022. **28**: p. 100365.

15. Zamora, M., R. Poranne, and S. Coros, *Learning solution manifolds for control problems via energy minimization.* IEEE Robotics and Automation Letters, 2022. **7**(3): p. 7912-7919.

16. Zhang, Y., et al., *Point stabilization of nonholonomic mobile robot by Bézier smooth subline constraint nonlinear model predictive control.* IEEE/ASME Transactions on Mechatronics, 2020. **26**(2): p. 990-1001.

17. Dong, D., et al., *Sampling-based learning control for quantum systems with uncertainties.* IEEE Transactions on Control Systems Technology, 2015. **23**(6): p. 2155-2166.

18. Li, J., et al., *A neural network approach to sampling based learning control for quantum system with uncertainty.* Communications in Computational Physics, 2021. **30**(5): p. 1453-1473.

19. Wolpert, D.H. and W.G. Macready, *No free lunch theorems for optimization.* IEEE transactions on evolutionary computation, 1997. **1**(1): p. 67-82.

20. Rizk-Allah, R.M. and A.E. Hassanien, *A movable damped wave algorithm for solving global optimization problems.* Evolutionary Intelligence, 2019. **12**: p. 49-72.

21. You, J.-Q. and F. Nori, *Atomic physics and quantum optics using superconducting circuits.* Nature, 2011. **474**(7353): p. 589-597.

22. You, J. and F. Nori, *Superconducting circuits and quantum information.* Physics today, 2005. **58**(11): p. 42-47.

23. Xiang, Z.-L., et al., *Hybrid quantum circuits: Superconducting circuits interacting<? format?> with other quantum systems.* Reviews of Modern Physics, 2013. **85**(2): p. 623-653.

24. Mabrok, M.A., et al. *Robust entanglement control between two atoms in a cavity using sampling-based learning control.* in *53rd IEEE Conference on Decision and Control.* 2014. IEEE.

25. Altomare, F., et al., *Tripartite interactions between two phase qubits and a resonant cavity.* Nature Physics, 2010. **6**(10): p. 777-781.

26. Bonnard, B., N. Shcherbakova, and D. Sugny, *The smooth continuation method in optimal control with an application to quantum systems.* ESAIM: Control, Optimisation and Calculus of Variations, 2011. **17**(1): p. 267-292.